Available online at www.sciencedirect.com
SCIENCE DIRECT®
International Journal of Solids and Structures 42 (2005) 3852–3866
INTERNATIONAL JOURNAL OF SOLIDS and STRUCTURES
www.elsevier.com/locate/ijsolstr

Crack nucleation from a single notch caused by stress-dependent surface reactions

Hong-Hui Yu *

Department of Mechanical Engineering, The City College of New York and the Graduate Center of the City University of New York, T218 Convent Ave at 140th Street, NY 10031, USA

Received 8 June 2004; received in revised form 11 November 2004
Available online 30 December 2004

Abstract

The surface of a solid under stress is unstable if there is mass exchange and transportation along the surface. A notch on the surface can be a preferred site for crack nucleation. This paper studies the evolution of a surface notch under stress dependant reaction. The surface is represented by a family of curves with many degrees of freedom, and the elastic field is solved using complex conformal mapping method. In the numerical simulations, the notch either deepens immediately and forms singular tip; or becomes perfectly flat after long time; or becomes blunter first, evolving slowly for a long time, then nucleates new surface instability and finally forms sharp tip; or becomes near flat first, then forms a bump on the surface. When the activation strain is small or the reaction is near equilibrium, the notch stability is mainly determined by the competition of strain energy and surface energy, and the sign of stress has little effect. When the surface reaction is away from equilibrium and activation strain is not small, stresses with different signs give totally different surface stability behaviors, depending on whether the solid is losing mass to or gaining mass from the environment.

Keywords: Crack nucleation; Surface reaction; Instability; Notch

1. Introduction

A surface under stress is unstable if mass can be exchanged and transported along the surface. Asaro and Tiller (1972) and others (Grinfeld, 1986; Srolovitz, 1989; Spencer et al., 1991; Freund, 1995; Gao, 1994) showed theoretically that a flat surface under a stress can evolve to a wavy shape by surface diffusion. The phenomenon of surface roughening has been observed in a growing number of experiments

* Tel.: +1 212 6506714; fax: +1 212 6508013.
E-mail address: ye@me.ccny.cuny.edu

0020-7683/$ - see front matter
doi:10.1016/j.ijsolstr.2004.11.010

(Yao et al., 1988; Cullis et al., 1992; LeGoues et al., 1990) and experiments involving controlled annealing have been used to test the characteristic length and time scales, as well as other features predicted in the theoretical models (Ozkan et al., 1997). Chiu and Gao (1993, 1995), and Yang and Srolovitz (1994) further showed that the wavy surface can evolve to form a sharp crack front. The process was observed by Jesson et al. (1993) on a surface of a strained epitaxial film.

A surface can also change its morphology by surface reaction, either by deposition or erosion. Srolovitz (1989) showed that a stressed surface is unstable due to evaporation/condensation. Hillig and Charles (1965) studied the crack nucleation from an elliptical notch due to stress-dependant surface reaction. Their theory is as follows. A notch pre-exists at the surface and the initial flaw is blunt. The solid loses mass to its environment by a surface reaction; the rate of the reaction depends on local stress. Because the stress along the flaw surface is non-uniform, the reaction may proceed faster at the flaw root than elsewhere, gradually changing the flaw into a sharp crack. Following the same general thought but using a linear kinetic law, Yu and Suo (1999) simulated the crack nucleation process for polycrystalline materials, in which grain boundaries cause surfaces to form grooves and further nucleate crack. Adopting a non-linear kinetic law in which the mobility depends on the applied stress, Yu and Suo (2000) and Liang and Suo (2001) studied the stability of a solid surface under small and large perturbations, respectively.

Delayed fracture, a brittle solid withstanding a static load for a long time and then breaking suddenly, has been studied for a long time. The dominant theory for delayed fracture, such as the work of Wiederhorn (1967) and others (Wiederhorn and Boltz, 1970; Lawn, 1974; Pollet and Burns, 1977; Johnson and Paris, 1968), is based on the framework of fracture mechanics and it has been successfully applied to components with relatively large initial crack sizes and short lifetimes. The theory assumes cracks pre-exist in the solid and slowly grow under chemical attack, assisted by stress. However, applying the theory to small components like glass fiber or microelectronic chips is inappropriate. For example, the instant breaking strength of a commercially available glass fiber, S-2 glass from Advance Glassfiber Yarns, LLC, is 4.9 Gpa at room temperature (Hartman et al., 1996). According to Griffith's fracture theory, the corresponding crack length is about $\frac{E\gamma_S}{\sigma_B^2}$, where γ_S, E, and σ_B are surface energy, Young's modulus and strength respectively. For $E = 89$ GPa, $\sigma_B = 4.9$ GPa, and $\gamma_S = 10$ J/m^2, the crack size is on the order of nanometer, which is too small to be called a crack. The delayed fracture of such small structure must involve the structural change in the solid over time to develop a stress concentration site. When the stress concentration is big enough, the solid may nucleate a crack by decohesion. The crack can further propagate under stress assisted chemical attack at the tip. There could be different mechanisms under different conditions for developing such a stress concentration site to have decohesion. The mechanism studied here is the stress-dependant surface reaction, as in Hillig and Charles (1965), Yu and Suo (1999), Yu and Suo (2000), Liang and Suo (2001).

This paper studies crack nucleation from a smooth notch on a stressed solid surface. The initial notch can be just a small perturbation or imperfection on the surface. The physical model adopted is similar to that of Hillig and Charles (1965). The main difficulty in analyzing the model is to determine the elastic field in a body with an evolving notch. Hillig and Charles (1965) approximated the elastic field by the solution for elliptic hole. Here, we solve the elastic field using conforming mapping method, representing the surface by a family of curves. The curves have many degrees of freedom and have the flexibility of describing complex shape, especially when the front of the notch becomes more and more localized.

Same as in Hillig and Charles (1965), Yu and Suo (2000) and Liang and Suo (2001), we adopt a non-linear kinetic law, in which the mobility of the reaction depends on stress. This effect is usually characterized by a quantity called activation volume, and has been applied in many systems (Aziz et al., 1991; Kao et al., 1988). It explains the different reaction rates and stability behaviors at solid surfaces under tensile and compressive stresses (Aziz et al., 1991; Kao et al., 1988; Barvosa-Carter et al., 1998; Shreter et al., 1999). In an experiment of a crystalline silicon immersed in an etchant, Shreter et al. (1999) observed the silicon surface developed crack-like defects under compression, but remained flat under tension.

In this paper, the physical aspects of the model are first outlined, and a family of curves to describe the boundary of the solid body is described next. The elastic field is solved analytically in Appendix A. After getting the dynamical system that used to evolve the structure, the paper finally presents the simulation results.

2. Physical description of the model

The physical model is similar to that in Hillig and Charles (1965) and Liang and Suo (2001). It is described here for self-containment. Fig. 1 illustrates the two dimensional model. The solid body is represented by a half plane and its surface by a curve. The surface tension of the solid immersing in the environment is γ_S, which is taken as isotropic. The solid and the environment, however, are not in equilibrium with each other: they exchange mass by dissolution, precipitation or chemical reaction. Denote g as the free energy increase per unit volume of solid deposited on a flat, stress-free surface. Within the environment, the molecular mobility is so large that the chemical potential is uniform and changes negligibly during the reaction. Thus, g is a constant in this model. The solid is subject to a remote stress σ_∞ in the horizontal direction, and remains elastic—that is, no dislocation or diffusional creep occurs to alleviate the stress concentration at the root of the notch. Furthermore, if condensation or precipitation occurs, mass attaches to the solid coherently, introducing no dislocations or pores.

As the surface reaction proceeds, the solid-environment as a system reduces its free energy. The displacement at the loading point is held fixed, so that the loading device does no work to the solid as the surface evolves. Let p be the free energy reduction associated with a unit volume of mass attached coherently to the solid surface. At a point on the surface, the local driving force is

$$p = g - w - \gamma_S \kappa, \tag{1}$$

where w is the strain energy density, and κ is the curvature of the surface. When $p > 0$, the solid gains mass at the point and when $p < 0$, the solid loses mass.

Let v_n be the reaction rate, namely, $v_n \mathrm{d}A$ is the volume of the solid gained at the element $\mathrm{d}A$ per unit time. Various functional forms of kinetic laws have been proposed on the basis of the transition state theory Hillig and Charles, 1965, 1988, 1998. In this paper, we adopt the following form:

$$v_n = v_0 \exp\left(\frac{-Q + \sigma\varepsilon^*\Omega}{kT}\right) \sinh\left(\frac{p\Omega}{2kT}\right). \tag{2}$$

The reaction is thermally activated. In Eq. (2), Q is the activation energy in the absence of the stress, k Boltsmann's constant, T the temperature, v_0 the pre-exponential factor, ε^* the activation strain, and Ω the volume per atom. $V^* = \varepsilon^*\Omega$ was called activation volume in Hillig and Charles (1965) and Kao et al. (1988). Under the normal stress in the tangential direction σ, the transitional complex is affected, and the activation energy changes to $Q - \sigma\varepsilon^*\Omega$.

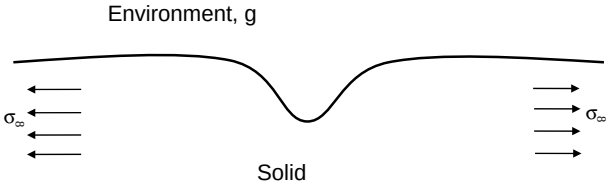

Fig. 1. A solid with a surface notch under stress. The solid is immersed in a large environment, which exchanges mass with the solid.

The characteristic length scale derived from the linear instability analysis (Asaro and Tiller, 1972; Grinfeld, 1986; Srolovitz, 1989; Spencer et al., 1991) is

$$l_0 = \pi E \gamma_S / \sigma_\infty^2 \tag{3}$$

representing the competition between the strain energy reduction and the surface energy increase associated with surface roughening. When the size of the notch is much bigger than l_0 or its curvature at the bottom of notch is $\ll 1/l_0$, we can treat the surface at the bottom of the notch as flat, and the analysis of Liang and Suo (2001) can be used. Here we deal with the notch with size comparable with or smaller than l_0.

3. Evolution equations

3.1. The surface representation

Conformal mapping

$$z = \lambda\left(\varsigma + \mathrm{i}\sum_0^n \frac{c_k i^k}{(\varsigma - i)^k}\right) \tag{4}$$

is used to transform the lower half of the complex plane, represented by $\varsigma = \xi + \mathrm{i}\eta$ with $\eta \leqslant 0$, into the solid body in the physical plane $z = x + \mathrm{i}y$. λ in Eq. (4) is a scaling factor and has a unit of length, representing the length scale of the notch width. The coefficients c_i's are real dimensionless numbers. c_0 gives the overall vertical position of the surface and c_1 to c_n describe the shape. The energy reference state is when the surface is free of stress and flat, $c_0 = c_1 = \cdots = c_n = 0$.

Let

$$r\mathrm{e}^{\mathrm{i}\psi} = -1 + \xi \cdot i, \tag{5}$$

where $\pi/2 < \psi < 3\pi/2$. The surface of the solid can be described by

$$x/\lambda = -\tan\psi - \sum_{k=1}^{n} c_k(-\cos\psi)^k \sin k\psi,$$

$$y/\lambda = \sum_{k=0}^{n} c_k(-\cos\psi)^k \cos k\psi. \tag{6}$$

At the bottom of the notch, $\psi = \pi$, and the depth is

$$d = \lambda\sum_{k=1}^{n}(-1)^k c_k. \tag{7}$$

Denoting $(\,)' = \mathrm{d}(\,)/\mathrm{d}\xi$, we have the first order derivatives along the surface,

$$x'/\lambda = 1 - \sum_{k=1}^{n} k c_k(-\cos\psi)^{k+1}\cos(k+1)\psi,$$

$$y'/\lambda = -\sum_{k=1}^{n} k c_k(-\cos\psi)^{k+1}\sin(k+1)\psi \tag{8}$$

and the second order derivatives

$$x''/\lambda = \sum_{k=1}^{n} k(k+1)c_k(-\cos\psi)^{k+2}\sin(k+2)\psi,$$

$$y''/\lambda = -\sum_{k=1}^{n} k(k+1)c_k(-\cos\psi)^{k+2}\cos(k+2)\psi. \tag{9}$$

The curvature along the surface is

$$\kappa = \frac{x''y' - x'y''}{(x'^2 + y'^2)^{3/2}}. \tag{10}$$

The normal velocity of the surface can be expressed in terms of $\dot{c}_i(= \mathrm{d}c_i/\mathrm{d}t)$,

$$v_n/\lambda = \sum_{k=0}^{n} A_k(\psi)\dot{c}_k, \tag{11}$$

where

$$A_k(\psi) = \frac{\lambda}{\sqrt{x'^2 + y'^2}}\left[(-\cos\psi)^k\cos k\psi - \sum_{j=1}^{n} jc_j(-\cos\psi)^{k+j+1}\cos(k-j-1)\psi\right]. \tag{12}$$

The coefficients c_0 to c_n are now the generalized coordinates of the system. The change of these coefficients over time gives the evolution of the surface. When singular tips form at the surface, $\omega'(\zeta) = 0$ has real solutions, and the curvature is infinite at the tips. As will be shown in the simulations, the conformal mapping represented by Eq. (4) allows the formation of multiple crack-like singular tips along the surface. This paper simulates the evolution of notch, especially the nucleation process of the crack-like singular tips, but not the subsequent decohesion and crack propagation process.

Though in this study we assume the geometric symmetry with respect to the middle of the initial notch, $x = 0$, the non-symmetric case can also be simulated by letting the coefficients c_k's be complex numbers.

3.2. Stress along the surface

As shown in the Appendix A, the conformal mapping allows the elastic field in the half plane bounded by the curves to be solved analytically. After lengthy derivation, the normal stress in the tangential direction along the surface is obtained,

$$\sigma_t = \sigma_\infty + 4\sigma_\infty\frac{x'\Delta_x + y'\Delta_y}{x'^2 + y'^2}, \tag{13}$$

where

$$\Delta_x = -\sum_{k=1}^{n} kd_k(-\cos\psi)^{k+1}\cos(k+1)\psi,$$

$$\Delta_y = -\sum_{k=1}^{n} kd_k(-\cos\psi)^{k+1}\sin(k+1)\psi. \tag{14}$$

The coefficients d_k $(k = 1,\ldots,n)$ are solved from Eq. (A.9) in the Appendix A. There is no traction applied on the evolving surface, so the strain energy density near the surface,

$$w = \sigma_t^2/2\overline{E}, \tag{15}$$

where $\overline{E} = E$ for plane stress problem and $\overline{E} = E/(1-\nu^2)$ for plane strain, with E the Young's modulus and ν the Poisson ratio.

3.3. The algorithm

Assume the surface configuration at time t is known. We need to find the new configuration after a time step Δt. The surface is discretized in the simulation. The normal velocity at all the discrete points, densely populated near the notch, can be calculated using the kinetic law, Eq. (2). Then, using Eq. (11), we search for $\dot{c}_i$'s that best fits the normal velocity at these discrete points, under a restriction on the energy dissipation rate.

Let m be the total number of discrete points on the surface. For a given $\psi_j = \pi/2 + j\pi/(m+1)$ $(j = 1, \ldots, m,\ m > n)$, Eq. (6) gives a corresponding point on the surface. The curvature at that point is calculated from Eq. (10), the stress state from Eq. (13), driving force from Eq. (1), and finally the normal velocity $v_{\mathrm{n}}^{(j)}$ is calculated from Eq. (2). Let matrix $\mathbf{A}$ have components A_{jk} being $A_k(\psi_j)$ in Eq. (12), Eq. (11) requires

$$\sum_{k=0}^{n} A_{jk}\dot{c}_k = v_n^{(j)}. \tag{16}$$

With finite degrees of freedom, the family of curves used here cannot exactly describe an arbitrary surface, and the above linear equation generally does not have an exact solution for $m > n$. The solution is sought to minimize the functional $\sum_{j=1}^{m}(\sum_{k=0}^{n} A_{\mathrm{jk}}\dot{c}_k - v_n^{(j)})^2$ and also to satisfy the condition that the energy dissipation per unit time, calculated by integrating the product of driving force in Eq. (1) and the normal velocity in Eq. (11), is the same if replacing Eq. (11) by Eq. (2),

$$\int_{-\infty}^{\infty} p\left(\sum_{k=0}^{n} A_k(\psi)\dot{c}_k\right)\mathrm{d}s = \int_{-\infty}^{\infty} pv_0 \exp\left(\frac{-Q+\sigma\varepsilon^*\Omega}{kT}\right)\sinh\left(\frac{p\Omega}{2kT}\right)\mathrm{d}s, \tag{17}$$

where $\mathrm{d}s = \sqrt{\mathrm{d}x^2 + \mathrm{d}y^2}$, with $\mathrm{d}x = -x'\,\mathrm{d}\psi/\cos^2\psi$ and $\mathrm{d}y = -y'\,\mathrm{d}\psi/\cos^2\psi$. The discrete form of Eq. (17) is

$$\sum_{k=0}^{n} q_k\dot{c}_k = \eta_k, \tag{18}$$

where

$$q_k = \sum_{j=1}^{m} p_j A_{jk}\frac{\sqrt{x'^2(\psi_j) + y'^2(\psi_j)}}{\cos^2\psi_j}\,\frac{\psi_{j+1} - \psi_{j-1}}{2}, \tag{19a}$$

$$\eta_k = \sum_{j=1}^{m} p_j v_n^{(j)}\frac{\sqrt{x'^2(\psi_j) + y'^2(\psi_j)}}{\cos^2\psi_j}\,\frac{\psi_{j+1} - \psi_{j-1}}{2}, \tag{19b}$$

where p_j is the driving force at ψ_j calculated from Eq. (1). The minimization criterion and the restriction lead to a set of linear algebra equations,

$$\sum_{k=0}^{n}\left(\sum_{j=1}^{m} A_{ji}A_{jk}\right)\dot{c}_k + q_i c_{n+1} = \sum_{j=1}^{m} v_n^{(j)}A_{ji}, \quad \text{for } i = 0 \text{ to } n, \tag{20}$$

where c_{n+1} is a Lagrange Multiplier.

Once $\dot{c}_0$ to $\dot{c}_n$ are solved from Eqs. (20) and (18), we integrate these derivatives with respect to time using Runge-Kutta method, to have new values of c_0 to c_n after a time step. The time step is determined automatically according to an error estimation scheme. The evolution of the surface profile over time is obtained by repeating the procedure.

4. Evolving a notch

To simulate the surface profile evolution using the kinetic law given by Eq. (2), we need the values of four dimensionless parameter groups,

$$\alpha = \frac{\sigma_\infty \varepsilon^* \Omega}{kT}, \quad \beta = \frac{\sigma_\infty^2 \Omega}{EkT}, \quad \chi = \frac{\gamma_S \Omega}{\lambda kT}, \quad \text{and} \quad \delta = \frac{g\Omega}{kT}. \tag{21}$$

If $\sigma_\infty = 100$ MPa, $\varepsilon^* = 0.1$, $\Omega = 10$ cc/mole, $T = 300$ K, $E = 100$ GPa, $\gamma_S = 1$ J/m^2, and $\lambda = 10^{-6}$ m, then $\alpha = 4 \times 10^{-2}$, $\beta = 4 \times 10^{-4}$, $\chi = 4 \times 10^{-3}$. δ is close to zero for system near equilibrium, and is a big number when the reaction is away from equilibrium. If the chemical energy reduction associated with reaction, g, is about 2.5 kJ per mole at 300 K, $\delta = 1$ for reaction gaining mass and -1 for losing mass. In the simulation, the unit time is

$$t_0 = \lambda / v_0 \exp(-Q/kT). \tag{22}$$

We assume the initial radius of curvature at the bottom of the notch is comparable to or smaller than l_0, given by Eq. (3), so that only one or just few singular tips can be nucleated from the notch.

According to the linear stability analysis based on Eq. (2) (Yu and Suo, 1999), when the reaction is near equilibrium, the stability of a flat surface is mainly determined by the competition of β and χ. Parameter β, corresponding to the strain energy, destabilizes surface, while χ, being related to the surface energy, resists surface roughening.

When reaction is far away from the equilibrium and $|\alpha| \gg \beta$, the surface stability is mainly determined by the sign of the stress. A positive α stabilizes the surface when the solid gains mass and destabilizes the surface when the solid loses mass. The effect of a negative α is the opposite. The strain energy term in Eq. (2) can compete with the first order term of stress when the stress concentration at the notch $K \approx \alpha/\beta - 1$.

4.1. Immediate singular tip nucleation

The first simulation is for $\alpha = 0.1$, $\beta = 0.005$, $\chi = 0.01$, and $\delta = 0$. This case will serve as a reference to show the effects of different controlling parameters in the simulations after. $\delta = 0$ means that the system is in equilibrium when the surface is perfectly flat, stress free and near equilibrium if the solid is stressed. In this simulation, the initial shape is given by $c_1 = 0.1$, $c_i = 0$, for $i \geqslant 2$, and its time sequence of evolution is shown in Fig. 2(a). The initial notch is shallow and smooth, unnoticeable when the scale of the figure is large. Since the applied load is large enough, the surface roughening driven by the strain energy reduction overcomes the surface smoothing effect by the surface energy. The notch sharpens under reaction, further magnifies the stress at the notch root and provides positive feedback for notch sharpening. Finally, a crack-like singular tip nucleates at the bottom of the notch. Fig. 2(b) plots the notch depth as a function of normalized time, for simulations with degrees of freedom of 4, 8, 12, 16 and 20. It shows that the numerical calculations are convergent even for this physically divergent problem.

4.2. Blunting first, then sharpening

Under the same conditions as the reference case, if the applied load is not large enough, the smoothing effect due to surface energy might overcome the roughening effect of the stress in the initial stage, so that the

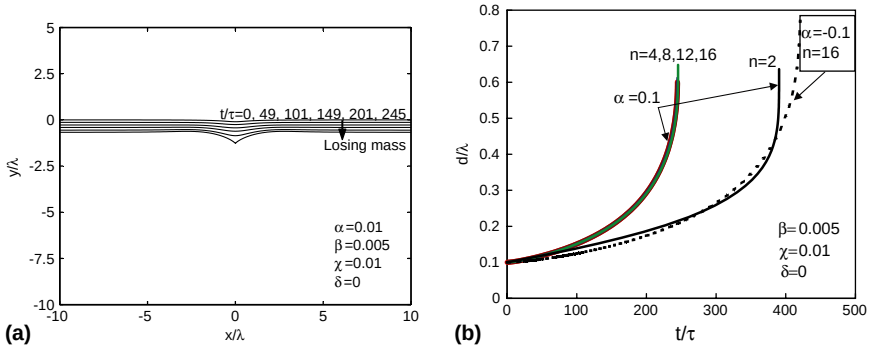

Fig. 2. Immediate notch deepening and singular tip formation for $\alpha = 0.1$, $\beta = 0.005$, $\chi = 0.01$ and $\delta = 0$, starting with $c_1 = 0.1$, and $c_i = 0$ for $i > 1$. (a) Solid surface profile evolution; (b) Notch depth as a function of normalized time.

depth of a preexisting notch decreases. On the other hand, from linear stability analysis, a flat surface is unstable under sinusoidal perturbation of long wavelength (Asaro and Tiller, 1972; Grinfeld, 1986; Srolovitz, 1989), so the notch depth would not decay forever: when the notch becomes wider and smoother, but before becomes totally flat, a new surface instability grows and finally a sharp tip can be nucleated.

In this simulation, we keep χ, δ, and the initial geometry be the same as the reference case but reduce the stress by half, so that $\alpha = 0.05$, $\beta = 0.00125$. Fig. 3(a) shows the time sequence of the surface evolution using degrees of freedom, $n = 20$. The notch first becomes blunter, the opening widens and the depth decreases, but after a long time, it becomes deeper and sharper again and finally nucleates singular tip. Fig. 3(b) plots the notch depth as a function of normalized time from simulations using different degrees of freedom, $n = 8$, 12, 16, and 20. All the simulations give the same results in the initial blunting process and the notch seems to approach to a constant depth. But if we wait for a long enough time, the notch depth starts to grow again, and finally the depth growing rate diverges. For the second stage of notching re-growing, simulations results are more sensitive to the number of the degrees of the freedom than those in the immediate sharpening cases. The situation is similar to the numerical tracing of a trajectory in a dynamical system which has a saddle point near the trajectory. For a given starting point, the initial evolving path either approaches to or moves away from the saddle point. In the former case, if the saddle point is close to the trajectory and the initial point is far way from the saddle point, the system approaches and gets close to the saddle point, slowly evolves near it because of small time derivatives, then accelerates and leaves. Since

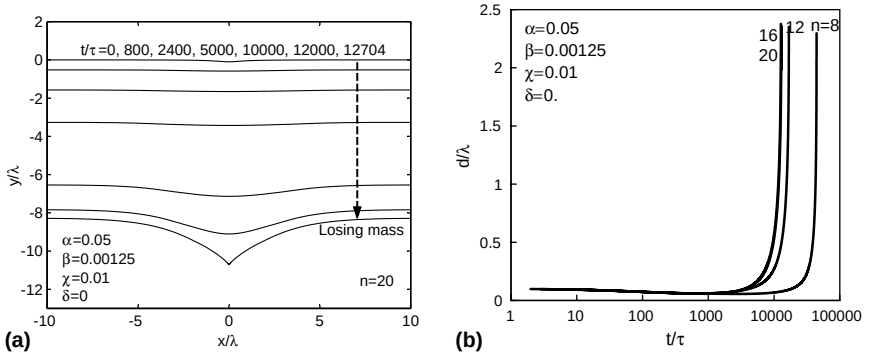

Fig. 3. Notch flattens first, then nucleates sharp tip, for $\alpha = 0.05$, $\beta = 0.00125$, $\chi = 0.01$ and $\delta = 0$, starting with $c_1 = 0.1$, and $c_i = 0$ for $i > 1$. (a) Solid surface profile evolution; (b) Notch depth as a function of normalized time.

it passes the neighborhood of the saddle point which is densely populated with many paths moving away, the results is more sensitive to the numerical scheme than in the case where the initial point is on the moving away branch of the trajectory. However, for a given initial point that is not on a path that hit the saddle point, when the accuracy control of the numerical scheme increases, the results will converge and the condition for convergence depends on the initial state. Such convergence can be seen in Fig. 3b. Except for the case starting with an unstable equilibrium state, such as a stressed flat surface, the evolution path depends on the initial geometry, energetics and kinetics of the system.

Using the same controlling parameters, Fig. 4 shows the simulation for a different initial geometry, with a sharper and deeper notch, $c_1 = 0.9$ and $c_i = 0$, for $i \geqslant 2$. The trend is the same as the previous simulations but time to nucleate a tip is different.

The simulations shown in Figs. 3 and 4 indicate that there is no absolute threshold stress under which there is no crack nucleation. As long as the external stress can destabilize a flat surface due to mass transport mechanisms, the surface will always nucleate crack no matter how small the stress is and what type of initial geometry starts with. However, it is still possible to define an 'immediate threshold stress' above which the notch will grow immediately and forms a crack, and below which the notch depth decreases first, then the notch becomes smoother and flatter, before developing new instability. One major difference between cases of immediate-sharpening and blunting-first-then-sharpening is the tip nucleation time. Since the latter one involves approaching to a slowly evolving, near steady state stage, singular tip nucleation requires much more time. For the cases in Figs. 2 and 3, the ratio of the remotes stresses is 2, but the ratio of the tip nucleate time is 1/53 (using $n = 16$ for both cases), though the initial notch is close to a flat surface. If the initial notch is deeper and sharper, the ratio of the two nucleation time becomes even larger. For example, when the initial geometry is $c_1 = 0.5$ and $c_i = 0$ for $i > 1$, under the same conditions, the time ratio is 1/807; and for an initial notch like in Fig. 4, if the load is doubled, the singular tip forms at the normalized time of 2.5×10^{-3} and the time ratio is $1/1.8 \times 10^{6}$. For this last case, we do not expect the immediate nucleation time to be accurate since when the stress concentration is very high, linear elasticity may not hold near the tip, so is the kinetic law. But the main point here is that when the initial notch is sharp, the two types of crack nucleation process involve totally different time scale. If the initial notch is not sharp, the final stage of dramatic sharpening and deepening only constitutes a small fraction of total lifetime.

An analogy exists in the instability of a flat surface under stress. From linear stability analysis in Asaro and Tiller (1972) for surface diffusion, a sinusoidal perturbation with wavelength longer than the critical value l_0 grows and perturbation with smaller wavelength decays in amplitude. However, perturbation with two sinusoidal waviness, whose wavelengths λ_1 and λ_2 are both smaller than l_0 may not vanish. Their

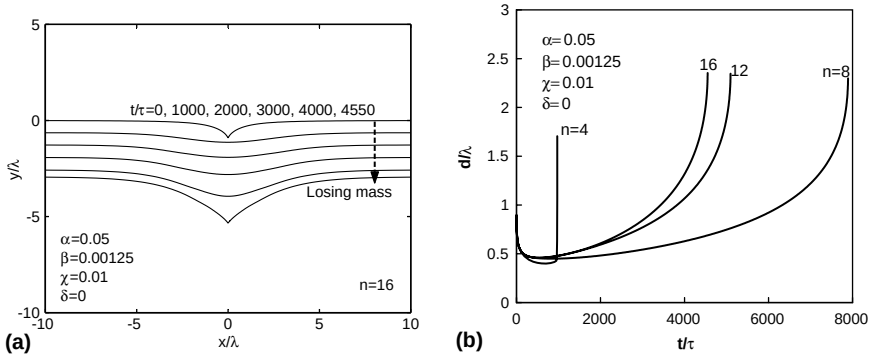

Fig. 4. Notch flattens first, then nucleates sharp tip for an initially deep notch, with $c_1 = 0.9$, and $c_i = 0$ for $i > 1$. The controlling parameters are $\alpha = 0.05$, $\beta = 0.00125$, $\chi = 0.01$ and $\delta = 0$. (a) Solid surface profile evolution; (b) Notch depth as a function of normalized time.

amplitudes do decay initially, but after some time, the higher order non-linear interactions among different sinusoidal modes would generate new modes with wavelengths $\lambda_1\lambda_2/(m\lambda_1 \pm n\lambda_2)$ (m and n are integers). Among these modes, those with wavelength greater than l_0 will grow and the surface becomes unstable. The process was illustrated by Coleman et al. (1995).

Another interesting observation is that when the load is smaller than the immediate threshold stress, the time to failure for a sharper and deeper notch, like the initial notch in Fig. 4b, might be longer than that for a shallow and smooth notch (depends on detailed shape), like the notch at $t = 1000$ or 2000 in the same figure. The result is based on the assumption that the remote stress does no work, for example, in the residually stressed surface. The conclusion should be still valid for thin film morphology change due to surface diffusion. Under annealing, a residually stressed thin film with many small cracks or notches on the surface might take longer time to break up into islands than those with a flat surface.

4.3. The effects of α and δ

When the reaction is far away from equilibrium, the driving force along the surface has the same sign everywhere and the surface stability is mainly determined by the stress induced mobility difference along the surface. Assume $\alpha > 0$, because of either tensile stress with positive ε^* or compressive stress with negative ε^*. When the solid is gaining mass by reaction, and $\alpha \gg \beta$, the reaction rate at the valleys of surface waviness is higher than that at the peaks, so the waviness starts to decay; and when the solid is losing mass by etching, the solid loses mass faster at the valleys than on the peaks, so the surface waviness will grow and the surface is unstable. The results is opposite for $\alpha < 0$ (see Chiu and Gao, 1993).

Fig. 5a shows the surface evolution for $\alpha = 0.1$, $\beta = 0.005$, $\chi = 0.01$, and $\delta = 1$. The solid gains mass and the reaction is away from equilibrium. The initial perturbation is large, represented by $c_1 = 0.85$ and $c_i = 0$ for $i > 1$. The notch depth decays as the average position of surface steadily moves up, and finally the surface becomes flat. According to linear stability analysis, the surface will remain flat forever. In Fig. 5a, in order to put surface profiles at far apart positions in the same plot, the vertical positions of the evolving surface have been shifted and indicated. The vertical axis in the figure gives the length scale in the vertical direction for comparing different surface morphology.

Under the same condition as in Fig. 5a, a case with $c_1 = 0.9$ was also simulated. Because the stress concentration is so high, the destabilizing effect of strain energy overcomes the stabilizing effect of the first order of stress, and the notch becomes a sharp tip in a very short time. From a simple analysis, when the reaction is far away from the equilibrium and $|\alpha| \gg \beta$, the effect of strain energy becomes significant when the stress concentration K at the bottom of the notch is bigger than $\alpha/\beta - 1$.

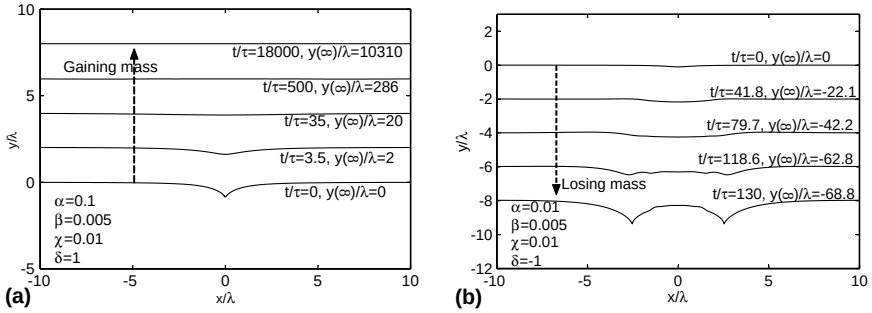

Fig. 5. Time sequences of surface profile evolution for reactions away from equilibrium, with $\alpha = 0.1$, $\beta = 0.005$, $\chi = 0.01$, and initial shape given by $c_1 = 0.1$, and $c_i = 0$ for $i > 1$. (a) $\delta = 1$, the solid gains mass; (b) $\delta = -1$, the solid loses mass.

Fig. 5b shows the case of losing mass, $\delta = -1$, with $\alpha = 0.1$, $\beta = 0.005$, $\chi = 0.01$. The notch depth grows immediately and two singular tips form in the end.

When α is negative, i.e., $\sigma\varepsilon^* < 0$, the effect is opposite when the reaction is away from equilibrium: stress stabilizes the surface when losing mass and destabilizes surface when gaining mass. If the reaction is near equilibrium, e.g., $\delta = 0$, the sign of α does not change the qualitative picture of surface evolution and the surface instability is mainly determined by the sign of the local driving force, i.e., the competition between the strain energy and surface energy. The dashed line in Fig. 2b is for the case of $\alpha = -0.1$, $\beta = 0.005$ and $\chi = 0.01$. It is similar to the case with positive α, except now sharp tip nucleation takes a little longer time.

When ε^* is small, the ratio of $\alpha/\beta = \varepsilon^*/\varepsilon$ becomes small. The term of the first order of stress in Eq. (2) becomes insignificant. Fig. 6a shows the surface profile evolution for solid gaining mass when the reaction is away from equilibrium with a small α, $\alpha = 0.001$. Other parameters are $\beta = 0.005$, $\chi = 0.01$, and $\delta = 1$, and the initial geometry is given by $c_1 = 0.1$ and $c_i = 0$ for $i > 1$. The solid gains mass. The notch first disappears due to the combined stabilizing effect of surface energy and the first order of stress, the surface becomes *near* flat but not totally flat for some time, slowly evolves and adjusts its shape, and finally new instabilities due to the destabilizing effect of strain energy start to occur at certain wavelength. Due to the limitation of the model, the simulation can only capture the instability near the original notch so that only the bump at the location of original notch is seen. The vertical positions of the surface profiles, indicated in the figure, have been shifted for easy viewing purpose. In Fig. 6b and c, all the parameters are the same as in Fig. 6a except $\delta = -1$ and 0, respectively. The surface is unstable from the beginning and tips nucleate in shorter time (Fig. 6b and c).

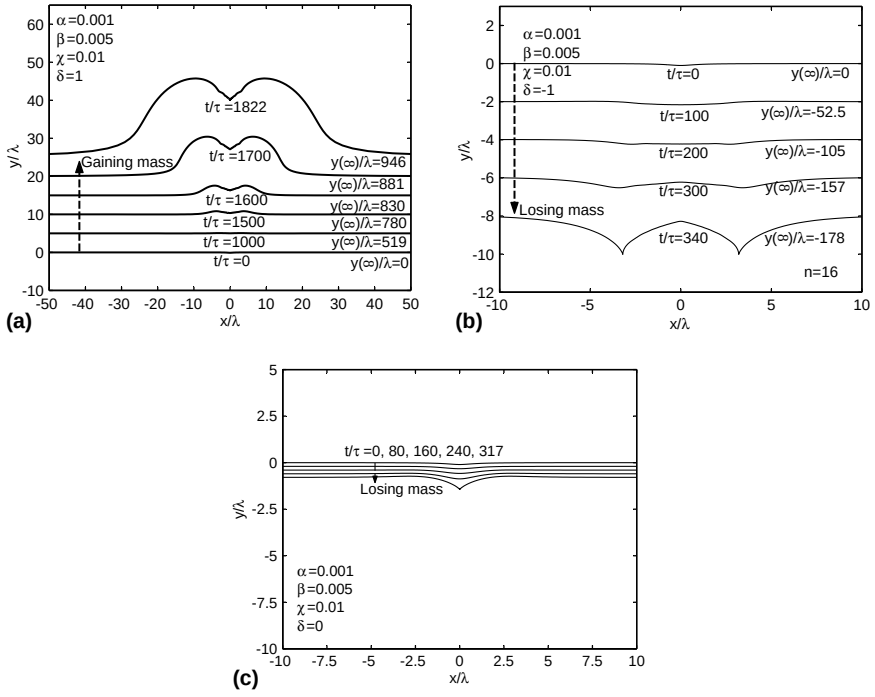

Fig. 6. Time sequences of surface profile evolution for the cases with small activation strain, $\alpha = 0.001$. Other parameters are, $\beta = 0.005$, $\chi = 0.01$ and the initial surface is given by $c_1 = 0.1$, and $c_i = 0$ for $i > 1$. (a) $\delta = 1$, the solid gains mass; (b) $\delta = -1$, the solid loses mass; (c) $\delta = 0$, the reaction is near equilibrium.

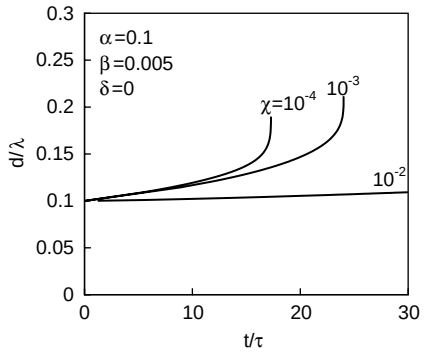

Fig. 7. Notch depth as a function of normalized time for cases with small χ, either due to small surface energy or large length scale, $\alpha = 0.1$, $\beta = 0.005$, $\delta = 0$, with initial shape given by $c_1 = 0.1$, and $c_i = 0$, $i > 1$.

4.4. The effect of χ

χ represents the resistance to surface roughening due to surface energy. Keep other parameters same as the reference case, $\alpha = 0.1$, $\beta = 0.005$ and $\delta = 0$, we change χ to 0.001 and 0.0001 in the last two simulations. Since the resistance to crack sharpening decreases, the sharp tip forms. Fig. 7 plots the notch depth as a function of the normalized time. For comparison, the curve for $\chi = 0.01$ (see Fig. 2) is also plotted. Besides small surface energy γ_S a long λ also gives a small χ. When λ is bigger, the length scale is bigger and the physical resolution of the simulation is lower, so the surface energy effect becomes insignificant in the calculation. In the present study, λ determines both the length and time scale.

5. Conclusion

This paper studies the evolution of a notch on a solid surface under stress dependant reaction. The elastic field is solved using a complex conformal mapping of many degrees of freedom. A dynamical system for evolving the surface is derived. The numerical simulations reveal the following. When the surface reaction is away from equilibrium and the activation strain is not small, a positive α would stabilize the surface when the solid is gaining mass and destabilizes the surface when losing mass. It is opposite for a negative α. When the activation strain is small or the reaction is near equilibrium, the surface stability is mainly controlled by the competition of strain energy and surface energy, and the sign of stress has little effect.

An initial notch can deepen immediately and form sharp tip in short time when the destabilizing effect of stress is large. In some cases, when the initial destabilizing effect of stress is small compared with the smoothing effect of surface energy, the notch depth first decreases, then, the surface evolves slowly near a quasi-steady state for a long time, and finally a new surface instability develops and sharp tips are formed on the surface. The simulations show that there is no absolute threshold stress beyond which the surface could nucleate crack. The threshold stress in practical application is related to time scale. The blunting first, then sharpening process takes much long time than the immediate crack nucleation. From the simulations, one can also see that the final stage of notch sharpening only constitutes a small fraction of total lifetime.

On may have concern if the surface representation used here can fully capture all the evolution paths, and thus if the general results derived are still valid. As any numerical method, the surface representation in Eq. (4) has only finite number of degrees of freedom. Within the family of surfaces that can be repre-

sented, a flat surface can keep flat if there is no initial perturbation or fluctuations, but it is neither an energy minimum state nor a maximum; it is a saddle point in the phase space of the dynamical system. Thus, the general feature for a saddle point is applicable and the qualitative conclusion derived, about the immediate sharpening or blunting-first-then-sharpening, is valid in general. The conclusion should be also hold for thin film morphology change due to surface diffusion. Recent numerical simulation (Liu and Yu, in press) using finite element method shows that, under annealing, a residually stressed thin film with many small cracks on the surface takes longer time to re-break up into islands than that a relatively flat surface having a small sinusoidal perturbation.

Acknowledgment

This work is supported by a grant from the Research Foundation of the City University of New York (RF-CUNY).

Appendix A. Elastic field in a half plane with a notch

We use the method of complex variables to solve the elastic field. In Fig. 1, the physical plane is (x, y). Define a complex variable $z = x + \mathrm{i}y$, where $\mathrm{i} = \sqrt{-1}$. Introduce another plane (ξ, η) and denote $\zeta = \xi + \mathrm{i}\eta$. The function

$$z = \omega(\varsigma) = \lambda\left(\varsigma + \mathrm{i}\sum_{0}^{n}\frac{c_k i^k}{(\varsigma - i)^k}\right) \tag{A.1}$$

maps the lower half of the ζ-plane to the area below the wavy boundary in the z-plane. In particular, the function maps the ξ-axis in the ζ-plane to the wavy boundary in the z-plane, as described by Eq. (6). λ in Eq. (A.1) is a scaling factor and has a unit of length, representing the length scale of the notch width. The coefficients c_i's are dimensionless, and can be treated as the generalized coordinates of the evolving surface. Before the surface forms any crack, $\omega(\zeta)$ is an analytic function in the lower half of the ζ-plane. When cracks form, the function loses analyticity, namely, equation $\omega'(\zeta) = 0$ has real solutions.

Any plane elastic field can be represented by two analytic functions $\phi(z)$ and $\rho(z)$. Written in terms of the two functions, displacements and resultant forces on the boundary are (Muskhelishvili, 1953)

$$\frac{E}{1+v}(u_x + \mathrm{i}u_y) = \kappa\phi - z\bar{\phi}'(\bar{z}) - \bar{\rho}(\bar{z}), \tag{A.2}$$

$$f_x + \mathrm{i}f_y = -\mathrm{i}\left[\phi + z\bar{\phi}'(\bar{z}) + \bar{\rho}(\bar{z})\right]. \tag{A.3}$$

Here E is Young's modulus and v Poisson's ratio; $\kappa = (3 - v)/(1 + v)$ for plane stress and $\kappa = 3 - 4v$ for plane strain. The notation $(\,)'$ stands for differentiation of a function with respect to its independent variable.

The two analytic functions are determined by boundary conditions. If the solid has perfectly flat surface, the elastic field is given by $\phi = \sigma z/4$ and $\rho = -\sigma z/2$. For the solid body with curved surface, we can write the complex functions as

$$\phi(z) = \frac{\sigma z}{4} + F(\zeta), \quad \rho(z) = -\frac{\sigma z}{2} + Y(\zeta), \tag{A.4}$$

where F and Y are the analytic functions representing the additional elastic field. The traction-free condition requires that the resultant force vanish. A combination of (A.1), (A.3) and (A.4) gives the boundary condition along the ξ-axis on the ζ-plane:

$$\bar{\omega}'(\xi)F(\xi)+\omega(\xi)\overline{F}'(\xi)+\bar{\omega}'(\xi)\overline{Y}(\xi)+\frac{\sigma}{2}\bar{\omega}'(\xi)[\omega(\xi)-\bar{\omega}(\xi)]=0. \tag{A.5}$$

The original elasticity problem now reduces to a problem of finding two functions $F(\zeta)$ and $Y(\zeta)$ that are analytic in the lower half of the ζ-plane, vanish as $|\varsigma|\to\infty$, and satisfy the boundary condition (A.5) along the ξ-axis.

Assume

$$F(\zeta)=\lambda\sigma\sum_{k=1}^{n}\frac{d_k i^{k+1}}{(\varsigma-i)^k} \tag{A.6}$$

and

$$\bar{\omega}'(\varsigma)\overline{Y}(\varsigma)=\lambda^2\sigma\sum_{k=0}^{2n+1}\frac{y_k(-i)^{k+1}}{(\varsigma+i)^k}, \tag{A.7}$$

where d_k's and y_k's are to be determined as functions of c_k's. Expand the left hand side of Eq. (A.5) with respect to $\varsigma=i$ to get Laurant series to the term of $1/(\varsigma-i)^n$, and get another series around $\varsigma=-i$ to the term of $1/(\varsigma+i)^{2n+1}$. By making the coefficients around these terms be zero, we obtain the linear equations about d_k's, and y_k's. Since the normal stress in the tangential direction along the evolving surface,

$$\sigma_{\mathrm{t}}=2Re\,\phi', \tag{A.8}$$

only involves $F(\zeta)$, we only need to solve the equations about d_k's, which are

$$\sum_{j=1}^{n}B_{kj}d_j=f_k, \tag{A.9}$$

where

$$B_{kj}=\delta_{kj}+\sum_{m=1}^{n-k}(-1)^{m+j}\frac{j(j+1)\cdots(j+m)}{m!2^{j+m+1}}c_{k+m}+(j\geqslant k)\sum_{m=1}^{n}(-1)^{j-k+m}\frac{m(m+1)\cdots(m+j-k)}{(j-k)!2^{m+j-k+1}}c_m$$
$$(\text{if } j\geqslant k) \tag{A.10}$$

and

$$f_k=-\frac{c_k}{2}-\sum_{m=1}^{n-k}\sum_{j=1}^{n}(-1)^{m+j}\frac{j(j+1)\cdots(j+m)}{m!2^{j+m+2}}c_jc_{m+k}. \tag{A.11}$$

Once d_k's are solved, y_k's can be solved from the equations derived from the coefficients of Laurant series around $\varsigma=i$. Since the results will not affect our calculation of stress near surface, they are not listed here.

On the surface of the current body, because the resultant force vanishes, a combination of (A.2) and (A.3) shows that the elastic displacements on the surface are given by

$$u_x+\mathrm{i}u_y=4\phi/E. \tag{A.12}$$

The above result is valid under the plane stress conditions; replace E by $E/(1-\nu^2)$ under the plane strain conditions.

References

Asaro, R.J., Tiller, W.A., 1972. Interface morphology development during stress-corrosion cracking. 1. Via surface diffusion. Metall. Trans. 3, 1789.

Aziz, M.J., Sabin, P.C., Lu, G.Q., 1991. The activation strain tensor–nonhydrostatic stress effects on crystal-growth kinetics. Phys. Rev. B 44, 9812–9816.

Barvosa-Carter, W., Aziz, M.J., Gray, L.J., Kaplan, T., 1998. Kinetically driven growth instability in stressed solids. Phys. Rev. Lett. 81, 1445–1448.

Chiu, C.H., Gao, H.J., 1993. Stress singularities along a cycloid rough-surface. Int. J. Solids Struct. 30, 2983–3012.

Chiu, C.H., Gao, H.J., 1995. A numerical study of stress controlled surface diffusion during epitaxial film growth. MRS Symp. Proc. 356, 33–44.

Coleman, B.D., Falk, R.S., Moakher, M., 1995. Stability of cylindrical bodies in the theory of surface diffusion. Physica D 89, 23–135.

Cullis, A.G., Robbins, D.J., Pidduck, A.J., Smith, P.W., 1992. The characteristics of strain-modulated surface undulations formed upon epitaxial $Si_{1-x}Ge_x$ alloy layers on Si. J. Cryst. Growth 123, 333–343.

Freund, L.B., 1995. Evolution of waviness on the surface of strained elastic solid due to stress-driven surface diffusion. Int. J. Solids Struct. 32, 911–923.

Gao, H.J., 1994. Some general properties of stress-driven surface evolution in a heteroepitaxial thin film structure. J. Mech. Phys. Solids 42, 741–772.

Grinfeld, M., 1986. Instability of interface between nonhydrostatically stressed elastic body and melts. Dokl. Akad. Nauk. SSSR 290, 1358–1363.

Hartman, D., Greenwood, M.E., Miller, D.M., 1996. High strength glass fibers, Technical papers, Available from: <http://www.agy.com/framesets/products/products.htm>.

Hillig, W.B., Charles, R.J., 1965. Surface, stress-dependant surface reaction, and strength. In: High strength materials. Wiley and Sons, New York, pp. 682–703.

Jesson, D.E., Pennycook, S.J., Baribeau, J.-M., Houghton, D.C., 1993. Direct imaging of surface cusp evolution during strained-layer epitaxy and implications for strain relaxation. Phys. Rev. Lett. 71, 1744–1747.

Johnson, H.H., Paris, P.C., 1968. Subcritical flaw growth. J. Eng. Fract. Mech. 1, 3–44.

Kao, D.B., McVittie, J.P., Nix, W.D., Saraswat, K.C., 1988. Two dimensional thermal oxidation of silicon—II. Modeling stress effect in wet oxides. IEEE Trans. Electron. Dev. ED-35, 25–36.

Lawn, B.R., 1974. Diffusion-controlled subcritical crack growth in presence of a dilute gas environment. Mater. Sci. Eng. 13, 277–283.

LeGoues, F.K., Copel, M., Tromp, R.M., 1990. Microstructure and strain relief of ge films grown layer by layer on Si(0 0 1). Phys. Rev. B 42, 11690–11700.

Liang, J., Suo, Z., 2001. Stress-assisted reaction at a solid–fluid interface. Interface Sci. 9, 93–104.

Liu, Z., Yu, H.H. On the stability of thin film under thermal annealing, in press.

Muskhelishvili, 1953. Some Basic Problems of the Mathematical Theory of Elasticity. P. Noordhoff Ltd., Groninger.

Ozkan, C.S., Nix, W.D., Gao, H.J., 1997. Strain relaxation and defect formation in heteroepitaxial $Si_{1-x}Ge_x$ films via controlled annealing experiments. Appl. Phys. Lett. 70, 2247–2249.

Pollet, J.-C., Burns, S.J., 1977. Thermally activated crack-propagation-theory. Int. J. Fract. 13, 667–679.

Shreter, Y.G., Tarkhin, D.V., Khorev, S.A., Rebane, Y.T., 1999. Instability of an elastically compressed silicon surface under etching. Phys. Solid State 41, 1295.

Spencer, B.J., Voorhees, X., Davis, S.H., 1991. Morphological instability in epitaxially strained dislocation free solid films. Phys. Rev. Lett. 67, 3696–3699.

Srolovitz, D.J., 1989. On the stability of surfaces of stressed solids. Acta Metall. 37, 621–625.

Wiederhorn, S.M., 1967. Influence of water vapor on crack propagation in soda-lime glass. J. Am. Ceram. Soc. 50, 407.

Wiederhorn, S.M., Boltz, L.H., 1970. Stress corrosion and static fatigue of glass. J. Am. Ceram. Soc. 53, 543.

Yang, W.H., Srolovitz, D.J., 1994. Surface-morphology evolution in stressed solids-surface-diffusion controlled crack initiation. J. Mech. Phys. Solids 42, 1551–1574.

Yao, J.Y., Anderson, T.G., Dunlop, G.L., 1988. Structure of lattice-strained Inxga1-Xas/Gaas layers studied by transmission electron microscopy. Appl. Phys. Lett. 53, 1420.

Yu, H.H., Suo, Z., 1999. Delayed fracture of ceramics caused by stress-dependent surface reactions. Acta Mater. 47, 77–88.

Yu, H.H., Suo, Z., 2000. Stress-dependent surface reactions and implications for a stress measurement technique. J. Appl. Phys. 87, 1211–1218.